Development of MCM-D Technology with Photosensitive Benzocyclobutene

Cristina B. Adamo[1], Alexander Flacker[1,2], Hercílio M. Cavalcanti[2,3,*], Ricardo C. Teixeira[1], Antonio L. P. Rotondaro[1] and Leandro T. Manera[2]

[1]Centro de Tecnologia da Informação Renato Archer - Campinas, Brazil
[2]Centro de Componentes Semicondutores, CCS, UNICAMP - Campinas, Brazil
[3]CI-Brasil Program, Brazil
e-mail: cristina.adamo@cti.gov.br

ABSTRACT

This paper evaluates and compares the development of Multi-Chip Module Deposited (MCM-D) technology using photosensitive benzocyclobutene (BCB) with the non-photosensitive BCB to fabricate passive devices. The polymer was used to isolate the metal/interconnection layers and also as the dielectric for the capacitors. Ni-P/Au was used as the conductor film and Ta_2N as the resistor film. The resistors' sheet resistance was measured with both transfer length method (TLM) and direct measurement while the measurements of the capacitors and inductors required the use of a Vector Network Analyzer (VNA) and some mathematical algorithms.

Index Terms: MCM-D; passive devices; photosensitive benzocyclobutene; thin films; RF characterization.

I. INTRODUCTION

Multi-chip module (MCM) is a technology for integrate multiple integrated circuits (ICs). There are three types of MCM: MCM-L-laminated; MCM-C-co-fired and MCM-D-thin films deposited [1, 2]. MCM-D technology is based on layers of dielectric and metals over a substrate that allows the fabrication of passive devices. Such devices work in the radiofrequency (RF) region and may function as external components for dies that can be assembled by wire-bonding and/or flip-chip techniques allowing the fabrication of very compact and highly integrated circuits [3, 4], i.e., MCM is very important due to the ability of producing interconnection between many dies on the same substrate.

Building blocks for MCM-D such as thin film deposition by sputtering, electroless and electrolytic deposition on alumina (Al_2O_3) substrates were available since the 1970's [5-7]. During the 1980's these procedures led to the development of the MCM-D technology that allowed the miniaturization of electronic systems and packaging and thus components with high interconnection density and better performance and reliability [8-10].

Today most of the passive components required in electronic systems are assembled as discrete components or passive arrays. In a very high density integration IC with discrete passive components, a lot of space is required for the realization of a single inductive, capacitive or resistive function [11, 12]. Even though such devices have similar frequency limitations when compared to implementations on silicon, since the parasitic effects are inherent to the construction of such devices, it is possible to achieve results comparable to what is found on state-of-the-art components, but with a much lower cost [13, 14].

There are several ways to assemble a MCM-D package. Variations include techniques on the films deposition, type of polymer (benzocyclobutene, polyimide) and metals (gold, copper) used and the layout of the devices to be produced [15].

Following the strategy of previous papers, [16, 17] MCM-D fabrication route was improved by introducing an insulation layer of BCB (photo or non photosensitive) over the Al_2O_3 substrate. This reduces the surface roughness and allows finer structures to be microfabricated while also reducing parasitic circuit elements that may limit device speed [18]. The sequence was also implemented using photosensitive benzocyclobutene polymer (p-BCB) which has the same physical and chemical properties as the non photosensitive BCB [19, 20] but can work just like a photoresist. The p-BCB improves the MCM-D process because the photosensitive material has no need of hard masks for via holes fabrication, thus reducing the amount of process steps and leading to a lower production cost.

The purpose of this study is to report the development of the MCM-D technology fabrication process using p-BCB to built passive devices that work in the radiofrequency (RF) region. The process includes microelectronic techniques such as vacuum deposition, photolithography, wet chemical etching and deposition.

II. EXPERIMENTAL

A. Fabrication technique process

Polished 99% Al_2O_3 (Coorstek) with dimension of 2.5 × 2.5 × 0.06 cm was used as substrates due to its properties of high thermal conductivity (20-35 W/m-k at 25 °C), high dielectric constant (9.9 at 1 MHz), low loss tangent (0.0001 at 1 MHz) and uniform density (3.87 g/cc) [21].

Firstly, the samples were cleaned by Extran 3% v/v in deionized water with ultrasonic bath. After that, one layer of BCB (Cyclotene 3022-35 Dow Company) was spin coated onto the blank cleaned substrate. This first film of polymer was applied to remove the parasitic influences of the substrate on the electrical measurement. The polymer was cured in an oven with an inert atmosphere (N_2) over constant temperature (250 °C) for one hour.

After that, thin films of Ta_2N, TiW and Au were sputtered (Sputron II-Balzers) onto the substrate without breaking the vacuum during the depositions. Ta_2N reactive deposition was performed at 200 °C (temperature of the substrate) by means of a Ta target etched by Argon (Ar) plasma in a N_2 atmosphere to produce the alloy. The base pressure for Ta_2N deposition was about 10^{-6} mbar, while partial pressures during deposition were 8×10^{-5} mbar for N_2 and 4×10^{-3} mbar for Ar. The sputtering was performed at 1.0 kV with depositions rate: 1.6, 1.0 and 18.2 Å/sec respectively for Ta_2N, TiW and Au.

After that, the samples had the Au layer thickened by a commercial solution of electrolytic gold (Auruna 553 - Umicore), at 70 °C with current density of 0.2 A/dm^2 and mechanical agitation. The final thickness of gold (sputtered + electrolytic) was 1,1 μm.

The passive components were fabricated by means of two photolithography process (Karl Suss MJB3) followed by wet etch. The first photolithography defines the passive components, while the second photolithography defines the resistors. All metals were etched using solutions and conditions as shown in Table I. After the etching process, samples were rinsed with deionized water (DI) and dried using N_2 and photoresist was removed with acetone, isopropyl alcohol and DI water.

In the sequence, the photosensitive p-BCB resin (Cyc1otene 4024-40 Dow Company) was spin coated at 5000 rpm for 30 sec. The physical, mechanical and thermal properties of p-BCB resin used are listed in Table II [20]. The properties of p-BCB, such as low dielectric constant and low dissipating factor, indicate that it is a good dielectric and insulator, minimizing the electrical energy loss and reducing parasitic capacitance. The viscosity, low water absorption, coefficient of thermal expansion and Tg > 350 °C makes p-BCB to be simple to operate, with low process temperature and thermal stability.

Table I. Film etch

Film	Solution	Temperature (°C)	Time (sec)
Ta_2N	$HF:HNO_3H_2O$ (1:4:4)	Room (~25)	20
TiW	H_2O_2 30% v/v	30	30
Au	Dip Gold 645 Umicore	40	45

Table II. Properties of photosensitive BCB resin (4024-40)

Dielectric constant	2.65 (1 kHz-20 GHz)
Dissipation factor	0.0008 (1 kHz-1 MHz)
Breakdown voltage (V/cm)	5.3×10^6
Volume resistivity (ohm-cm)	1×10^{19}
Stress (MPa)	28 ± –2
Water absorption (%)	< 0.25
Tg (°C)	> 350
Coefficient of thermal expansion (ppm/°C)	52
Viscosity (cSt, 25°C)	350

After exposure, the development of p-BCB occurs by using DS 3000 at 35 °C for a few minutes. In the sequence the sample was rinsed in DS 3000 at room temperature and dried in spinner with N_2. The polymer was cured under the same experimental conditions as the first BCB layer. The cured film was descummed using a reactive ion etch (RIE) plasma process with O_2/SF_6 (chamber pressure: 50 mTorr; plasma power: 500 W; plasma time: 15 minutes; SF6 and O2 flow rate: 10 sccm), in order to clean the vias and remove the thin layer of polymer residues left during the developed process.

In the sequence, another plasma treatment is necessary to improve metal adhesion on the p-BCB surface. Plasma conditions for adhesion improve are: 10 sccm O_2, pressure of 200 mTorr, power density of 100 W for 10 minutes.

The vias were then filled with electroless NiP [22] (after treatment with stannous and palladium ions) and electrolytic Au. Another photolithography process and wet etch were performed to produce the pads.

The thicknesses of the films deposited for the MCM-D procedure described in this paper are presented on Table III below.

Table III. Thickness of the films

Film	Thickness (nm)
BCB (first layer)	1500
Ta_2N	120
TiW	30
Au (sputtering)	100
Au (electrolytic)	1000
BCB (second layer)	4000

B. Comparative process of p-BCB and BCB

Fig. 1 shows the different technological steps between photo and non-photo BCB.

In MCMs, vias are used to interconnect many conductors layers, so via formation is a fundamental step for this technology. Photosensitive BCB is a negative polymer (unexposed areas are removed during solvent development) and its processing is very similar to a generic photolithographic process [23].

Fig. 2 compares process flows for via formation using photo and non photo sensitive BCB. It is clear that the process is simplified with p-BCB. Non-photosensitive BCB needs an extra metal deposition/etching and photoresist spin steps to be used as hard mask, which is not necessary for p-BCB.

As shown here, the use of photosensitive materials leads to a reduction of the amount of process steps. It makes unnecessary the use of photoresist, re-

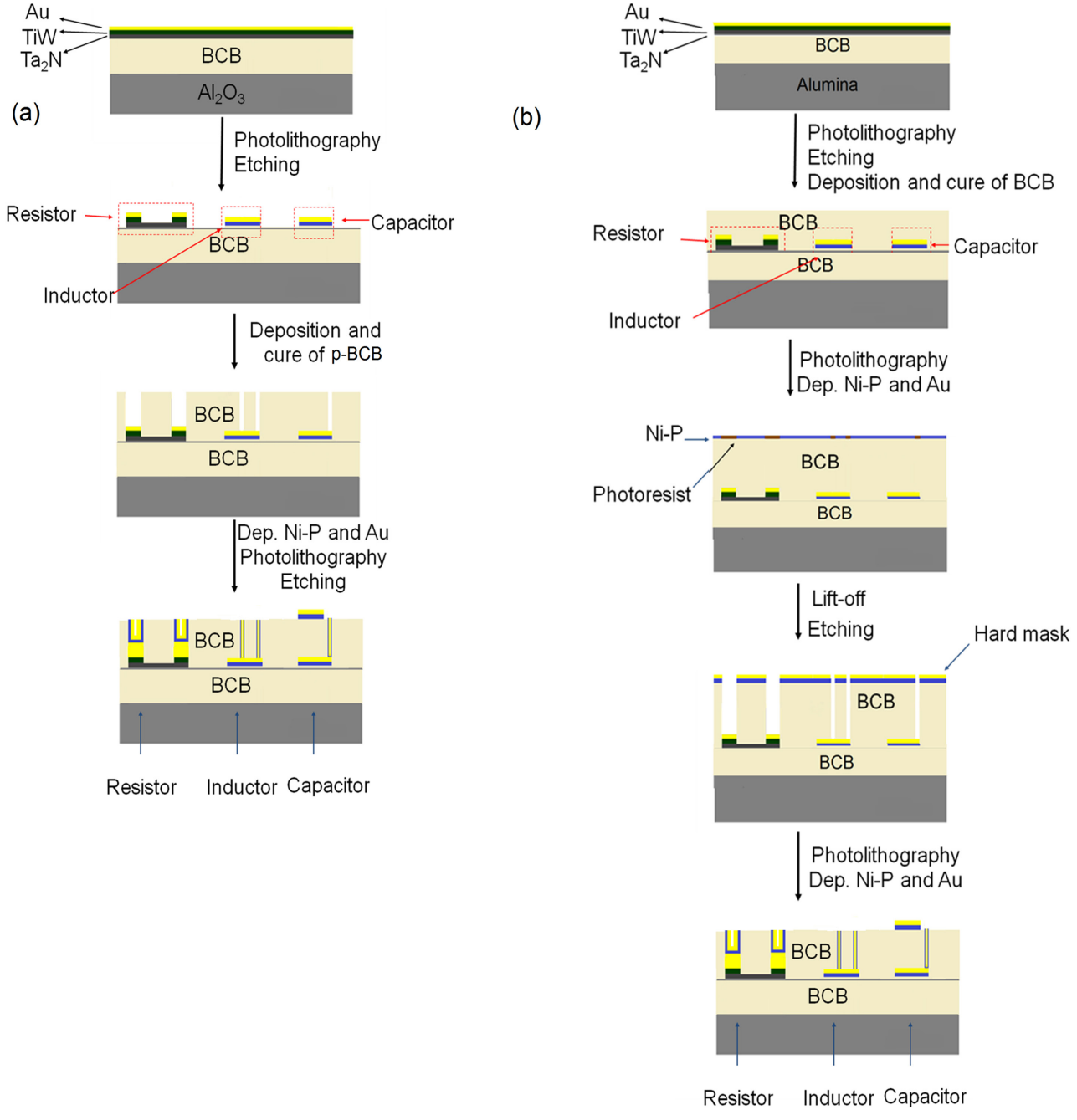

Figure 1. Fabrication steps summary using (a) p-BCB and (b) BCB (not in scale)

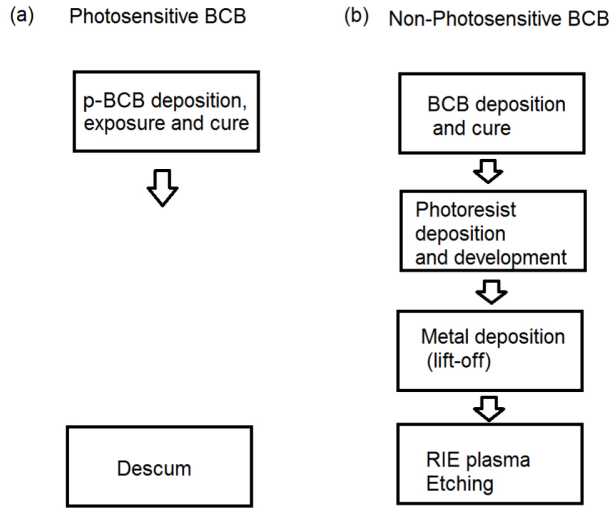

Figure 2. Diagram comparing the via formation process for non-photosensitive and photosensitive BCB

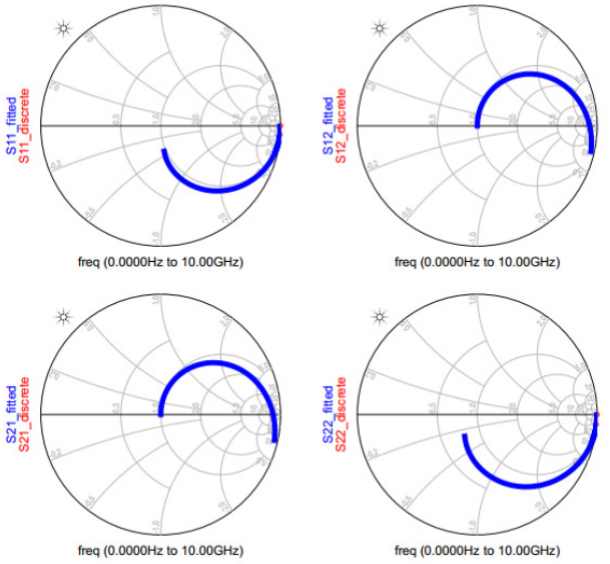

Figure 3. Example of a Smith chart plot on ADS with S-parameters matrix measured for one capacitor. The blue and red curves (overlapped in this plot) represent a momentum simulation (electromagnetic) comparison between a discrete and a fitting data simulation

duce process cycle time, saves material and labor and lower final cost. Thus, it is desirable to use photosensitive material for low cost manufacturing.

C. Measurement and data acquisition strategy

Electrical measurements on resistor were performed in a microprobe station attached to an HP4145-B while capacitors and inductors used a Vector Network Analyzer (VNA) HP8510-C. Probes are GSG Cascade and adequate for measurements on Au metal pads. In the case of inductors and capacitors a 2-port scattering parameters (S-parameters) matrix is obtained for each device as an .s2p file. The data is interpreted by means of Keysight's Advanced Design Systems (ADS) software [24]. The s-parameters data obtained from the VNA may be plotted in ADS as a Smith chart by simply loading the .s2p files (Fig. 3). In order to obtain the capacitance and inductance of the devices, it is necessary to treat the s-parameters data. First, the s-parameters matrix is converted to z-parameters and then to a one-port model. The result is the impedance of the device. Finally, the capacitance C and inductance L are derived from its impedance equations ($C = 1/\omega Z_c$ and $L = Z_L/\omega$). Equations (1-5) show how the data acquisition procedure [25] is implemented in ADS.

$$\omega = 2 \times \pi \times f \quad (1)$$

$$Z_{M,\,2p} = \text{stoz}(s) \quad (2)$$

$$Z_{2p\text{-to-}1p} = Z_{M,\,2p}(1,1) - 2Z_{M,\,2p}(1,2) + Z_{M,\,2p}(2,2) \quad (3)$$

$$L_{eff} = Z_{2p\text{-to-}1p}/\omega \quad (4)$$

$$C_{eff} = 1/\omega \times Z_{2p\text{-to-}1p} \quad (5)$$

Where,
stoz(s) = transforming matrix, from s to z parameters;
2p-to-1p = transforming equation from 2 port parameters to 1 port;
L_{eff} = Effective inductance;
C_{eff} = Effective capacitance;

III. RESULTS AND DISCUSSION

A. Resistors

Ta_2N is used as the main material for the resistor. The sheet resistance was obtained by the slope of the resistance *vs.* number of squares plot, which also gave the value of the contact resistance (intercept), and by the direct measurement with a voltmeter over a test wafer with 42 resistors (Fig. 4).

Fig. 5a show the Transfer Length Method (TLM) results [26] and Fig. 5b shows results of individual resistors. Fig. 6 shows the tridimensional layout of one resistor

Table IV summarizes all resistance values obtained. It can be observed that the values from different techniques/devices are in agreement. The slight difference could be related to the measurement technique or to some problems that could have occurred during processing such as overetch (that changed the original layout) or the presence of impurities.

Another important aspect of the fabricated resistor is the low temperature coefficient (Fig. 7), when compared to the usual values of integrated resistors.

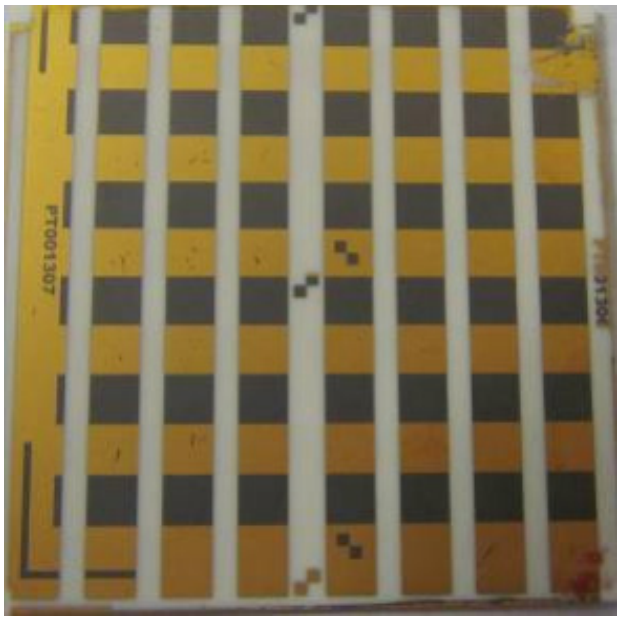

Figure 4. Fig. 4 Test wafer for direct measurement of sheet resistance; each square/resistor is 2 mm long

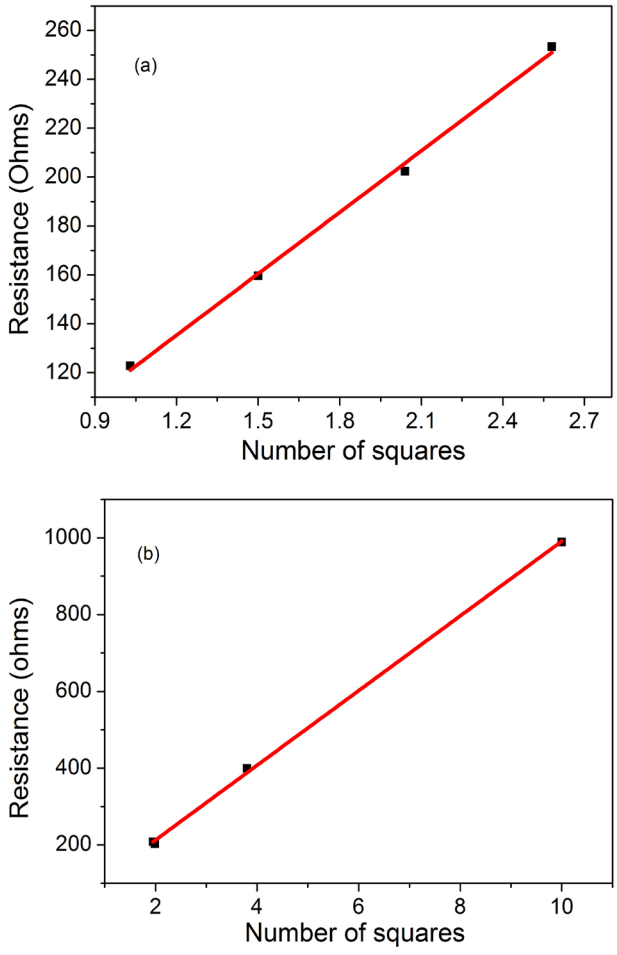

Figure 5. Resistance measured in (a) TLM and (b) resistors

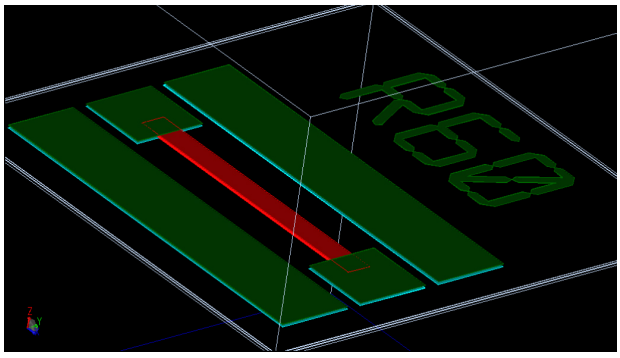

Figure 6. 3D layout of resistor; width: 50 mm, length: 500 mm, PAD: 150 mm × 150 mm

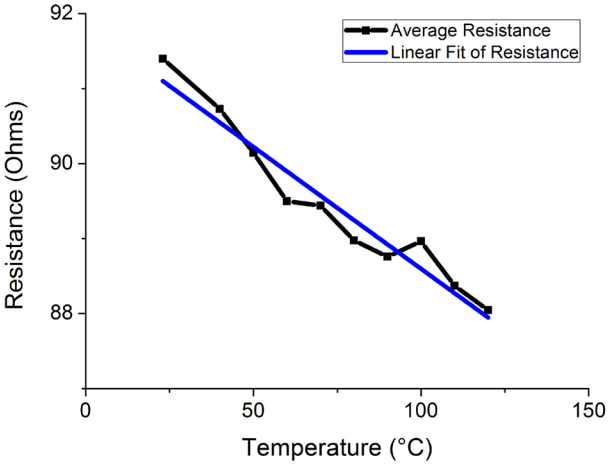

Figure 7. Resistance vs. temperature

Table IV. Value of resistances

	Sheet resistance (Ω/□)	Contact resistance (Ω/□)	Resistivity Ta_2N (mΩ/cm)
Rs-graphic-TLM	84 ± 3	17 ± 2	1.00
Rs-graphic-resistors 100	97 ± 2	18 ± 9	1.16
Rs-resistance voltmeter	91 ± 5	–	1.09

This makes possible for designers to have reasonable stability over temperature for current and voltage references, for example. It was observed that the temperature coefficient is negative and has a value of about -0 mΩ/ºC or 0.04%/ºC variation when compared to the nominal resistance value at 23 °C.

B. Capacitors

The metal-insulator-metal (MIM) capacitors have BCB as the dielectric and Au as the conductor. Two capacitor layouts, round and square, were tested (Fig. 8).

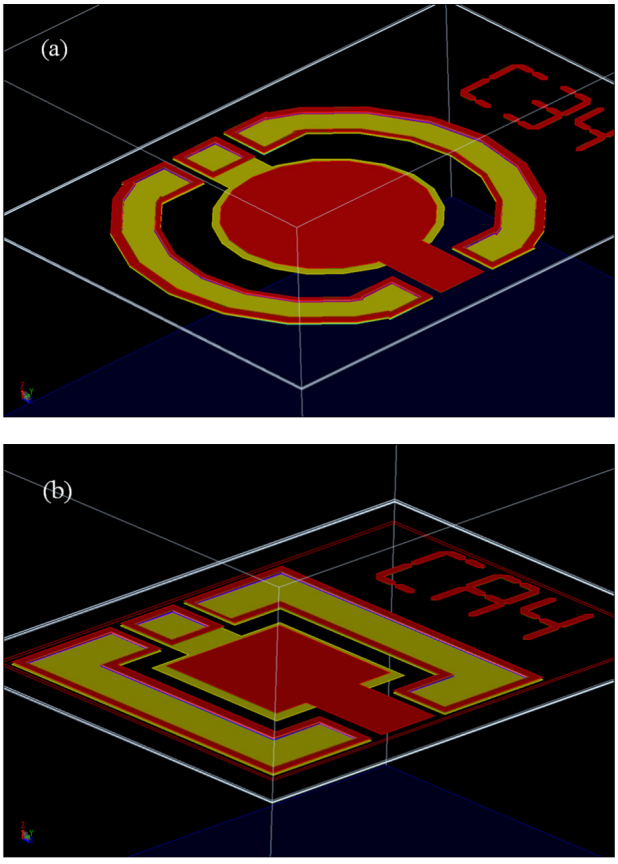

Figure 8. Fig. 8 Capacitor layout types (a) type I and (b) type II

Electrical behavior of the capacitors was measured for frequencies from 45 MHz to 10 GHz. The capacitance of each device is described as a function of frequency on Fig. 9. Table V contains information about each device and the capacitance at the center frequency of three of the main Industrial, Scientifical and Medical (ISM) bands [27]. These frequencies were chosen because there are many applications for them, since they are license free frequencies.

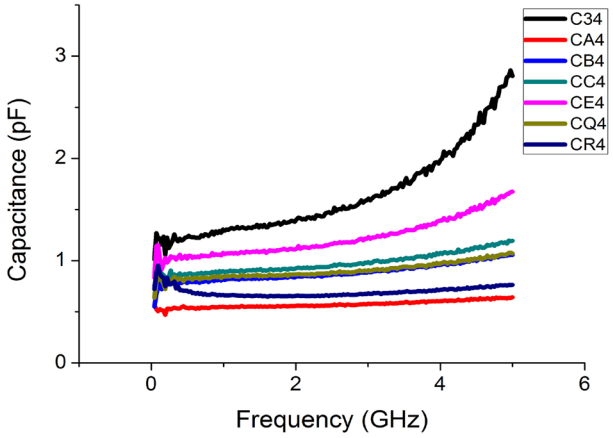

Figure 9. Fig. 9 Result of capacitance vs. frequency

Table V. Capacitors data

Capacitor	Dimension (μm)	Capacitance (pF) 433.92 MHz	915 MHz	2.45 GHz	Capacitance *per* area (pF/mm²)
C34	r = 280	1.20	1.27	1.47	5.97
CA4	325 × 325	0.55	0.55	0.56	5.30
CB4	400 × 400	0.79	0.80	0.85	5.31
CC4	425 × 425	0.86	0.87	0.94	5.20
CE4	475 × 475	1.02	1.05	1.15	5.10
CQ4[1]	400 × 400	0.81	0.84	0.87	5.44
CR4[1]	425 × 425	0.71	0.66	0.66	3.65

[1]Capacitor CQ4 and CR4 have the same layout as capacitors CB4 and CC4, respectively, except that they are positioned on the periphery of the wafer.

Capacitors were designed having the lower plates slightly larger than the upper one, in order to avoid misalignment problems during the fabrication process.

Some of the main constraints for the capacitance of these devices are area and dielectric constant. The choice for BCB as the dielectric is justified as this material has a relative electric permittivity constant of about 2.6 and it is a very stable material, with low sensitivity to moisture and temperature variations [19]. The thickness of BCB should be the same in all capacitors (4 microns), but some differences are found due to the border effect. The capacitance *per* area was found to be ca. 5 pF/mm², except capacitor CR4.

C. Inductors

The inductors were fabricated having three different layouts (Fig. 10). The resonant frequency of each device is about 6 GHz. The inductance as a function of frequency was obtained with the procedures described before and the results obtained are shown on Fig. 11. Inductors require a more delicate design procedure when compared to capacitors due to complex relationships between the magnetic and electric field going through these devices.

For instance, the inductance is higher with a greater number of loops, but this also implicates on a worse quality factor. Therefore, the design of this device must take a careful procedure from both the design and manufacture process teams. The main constraints for this device are area, inductance and quality factor.

It was not observed any correlation between the inductor layout type and the quality factor, thus resulting in a quality factor of a few units, probably because the thickness of the conductor metal should be thicker. Finally, the main characteristics of the fabricated inductors are described on Table VI.

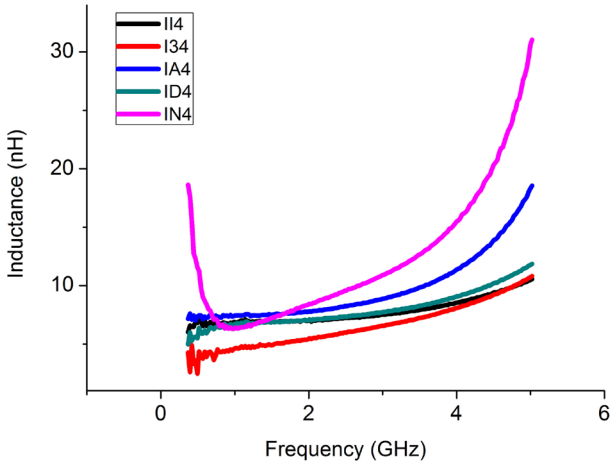

Figure 11. Inductance vs. frequency

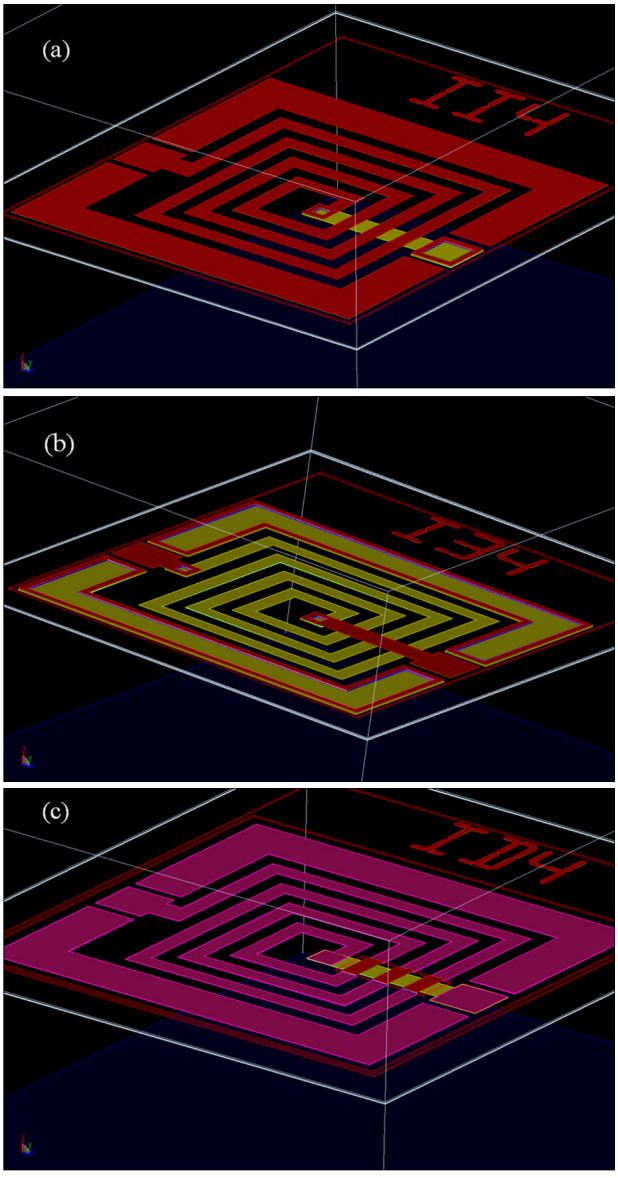

Figure 10. Fig. 10 Inductors layout types (a) type I; (b) type II and (c) type III

Table VI. Inductors data

Inductor	Dimension[1] (μm × μm)	Inductance (nH) 433.92 MHz	915 MHz	2.45 GHz
II4	1122 × 1000	6.48	6.64	7.20
I34	770 × 765	4.30	4.39	5.91
IA4	840 × 840	7.20	7.35	8.18
IN4	915 × 915	14.49	6.31	9.46
ID4	865 × 865	5.43	6.56	7.30

[1]The dimension includes the guard ring.

IV. FUTURE APPLICATIONS

Further development of the MCM-D technology presented on this work will be done by means of a chain of many different initiatives by both the design and fabrication process teams. An important contribution was to calibrate the model of the devices by using the data obtained from each device and build a technology file and a substrate description for the 3D geometrical description on the ADS platform.

With this it was possible for the design team to run accurate 3D electromagnetic simulations in order to preview the electrical behavior of the fabricated devices prior to its physical implementation. The modeling will be done simulating the "substrate" of our technology in the ADS, and finding a set of equations that could predict the operation of the devices in the RF. Once the simulations are well calibrated, it will be possible to run optimizations on the devices for a new set of masks, having devices with improved electrical and geometrical characteristics such as quality factor (for inductors) and capacitance per area ratio (for capacitors). Then, it will be possible to build up filters from the basic devices and verify its electrical behavior over a wide range of frequency.

On the process side, it will be researched new materials to work as barrier (as a replacement of TiW) in order to grant a better soldability for wirebond. It will also be evaluated the possibility of changing some parameters in the fabrication process (such as: temperature, thickness, etc.) in order to achieve a better quality factor for the inductors and a better capacitance for the capacitors.

V. CONCLUSIONS

The development of MCM-D technology with photosensitive BCB was proved to be effective in the production of passive devices on alumina substrate. The components were successfully produced and it was observed a very good electrical behavior with capacitors and inductors having its respective capacitance and inductance values in accordance for the GHz applica-

tions which makes possible the usage of the technology for many different RF applications such as that on ISM bands of up to 2.45 GHz. Resistance measured by different methodologies showed a good correlation of values. Although the components have good performance, the technology allows different modifications to be tested in order to improve the technique and include the fabrication of different RF devices.

ACKNOWLEDGMENTS

The authors would like to acknowledge CTI Renato Archer (DEE, DMS and DAPE), CCS-UNICAMP, CNPq, FAPESP, FINEP, CNPEM (LNNano), CI-Brasil and INCT Namitec.

REFERENCES

[1] P. Gerlach, C. Linder, and K.-H. Becks, "Multi chip modules technologies," *Nucl. Instrum. Methods Phys. Res., Sect. A* vol. 473, 2001, pp. 102-103.

[2] N. A. Blum, H. K. Charles Jr., and A. S. Francomacaro, "Multichip module substrates," *Johns Hopkins APL Tech. Dig.,* vol. 20, 1999, pp. 62-69.

[3] S. Bhagath, and P. Lall, "An overview of multichip modules," *Solid State Technology*, 1993, pp. 65-73.

[4] P. Pieters, S. Brebels, E. Beyne, and W. Raedt, "Advances in the microwave MCM-D technology," *Microelectron. Int.*, vol. 17, 2000, pp. 19-22.

[5] A. Flacker, C. A. Finardi, A. M. Almeida, P. Molina, and M. Barnett, "Tecnologia de baixo custo para placas de alta densidade de interconexão," *Tratamento de Superfície*, no. 88, 1998, pp. 28-33.

[6] A. Flacker, A. C. Pagotto, A. Gozzi, A. de Almeida, C. Finardi, J. Molina, M. dos Santos, and M. Barnett, "An innovative and low cost deposition technology applied to MCM-D fabrication," *Journal of Solid State Devices and Circuits*, vol. 6, 1996, pp. 7-11.

[7] C. Cabreira, A. Flacker, S. D. Yamamoto, E. A. Gomes, M. Canesqui, and J. Swart, "Tecnologia MIC aplicada a dispositivos de RF," in *Simpósio Brasileiro de Microondas e Optoeletronica*, 2006, Belo Horizonte.

[8] J. Tang, X. Sun, and L. Luo, "A wafer level multi-chip module process with thick photosensitive benzocyclobutene as the dielectric for microwave application," *J. Micromech. Microeng*., vol. 21, 2011, pp. 1-8.

[9] T. S. Kim, and G. S. Gary "Time series modeling of photosensitive polymer development rate for formation application," *IEEE Trans. Electron. Packag. Manuf*., vol. 25, 2002, pp. 203-209.

[10] J. Grzyb, D. Cottet, and G. Troster, "Integrated passive elements on low cost MCM-D substrates," in *Proceedings of International Conference on High-Density Interconnect and Systems Packaging*, 200l, pp. 256-261.

[11] J. Dougherty, "The Nemi roadmap: integrated passives technology and economics," *Proceedings of the Capacitor and Resistor Technology Symposium* (Carts), Scottsdale, April 2013.

[12] C. B. Adamo, A. Flacker, W. Freitas, R. C. Teixeira, M. O. Silva, and A. L. P. Rotondaro, "Multi-chip module (MCM-D) using thin film technology," *Journal of Integrated Circuits and Systems*, vol. 10, no. 1, 2015, pp. 21-29.

[13] K.K.Samanta,"Multilayerthick-filmandnextgenerationcost-effective millimetre-wave SoP circuit and system integration techniques," *2015 IEEE MTT-S International Microwave and RF Conference (IMaRC)*, Hyderabad, Dec. 2015, pp. 393-395. doi: 10.1109/IMaRC.2015.7411446.

[14] M. A. Al-Alaoui, "Novel stable higher order-to- transforms," *IEEE Trans. Circuits Syst.*, vol. 48, no. 11, Nov. 2001, pp. 1326-1329.

[15] P. Pieters, W. D. Raedt, and E. Beyne, "MCM-D technology for integrated passives components," *IEEE Microelectronics*, 1999, pp. 137-140.

[16] W. Freitas, A. Flacker, C. B. Adamo, and A. L. P. Rotondaro, "Development of Multi-Chip Module-D technology-testchip," *IEEE Microelectronics Technology and Devices*, 2013, pp. 1-4.

[17] C. B. Adamo, A. Flacker, W. Freitas, R. C. Teixeira, M. da Silva, and A. L. P. Rotondaro, "Multi-chip module (MCM-D) using thin film technology," in *IEEE Symposium on Microelectronics Technology and Devices*, 2014, pp. 1-4.

[18] L. B. Zoccal, S. D. Yamamoto, C. M. Cabreira, A. Flacker, E. A. Gomes, J. A. Diniz, and J. W. Swart, "RF passive components in MCM-D," in *SBMO/IEEE MTT-S International Microwave & Optoelectronics Conference (IMOC)*, 2007, pp.122-126.

[19] "Cyclotene processing procedures for cyclotene 3000 series dry etch resins," *Dow Tech. Rep*., 2005, pp. 1-8.

[20] "Cyclotene processing procedures for cyclotene 4000 series photo BCB resins," *Dow Tech. Rep*., 2005, pp. 1-8.

[21] "Thick-Film ceramic substrates design guide", *Coorstek Tech. Rep.*, 2008, pp. 14.

[22] C. D. M. Campos, A. Flacker, S. A. Moshkalev, and E. G. O. Nobrega, "Comparative analysis of thin Ni and CoNiMnP magnetic films," *Thin Solid Films*, vol. 520, 2012, pp. 4871-4874.

[23] T. S. Kim, and G. S. May, "Time series modeling of photosensitive polymer development rate for via formation applications," *IEEE Trans. Electron. Packag. Manuf.*, vol. 25, no. 3, 2002, pp. 203-209.

[24] Keysight ADS site. [Online]. Available: http://www.keysight.com/en/pc-1297113/advanced-design-system-ads'?cc=BR&1c=por

[25] D. A. Frickey, "Conversions between S, Z, Y, h, ABCD, and T parameters which are valid for complex source and load impedances," *IEEE Trans. Microwave Theory Tech*., vol. 42, 1994, pp. 205-211.

[26] Contact resistance and TLM measurements. [Online]. Available: http://tuttle.merc.iastate.edulee432/topics/metals/tlm_measurements.pdf

[27] RF BASICS - Texas Instruments lecture note. [Online]. Available: http://www.ti.comllitiml/swrp082/swrp082.pd